Laser and Particle Beams (2012), *30*, 207–213.

doi:10.1017/S026303461100084X

Study of stimulated Brillouin scattering in extended paraxial region

PRERANA SHARMA,[1] A.K. BHARDWAJ,[2] AND R.P. SHARMA[3]

[1]Physics Department, Ujjain Engineering College, Ujjain, India
[2]N. S. C. B. Government Post Graduate College, Biaora, India
[3]Centre for Energy Studies, IIT, New Delhi, India

(RECEIVED 26 August 2011; ACCEPTED 4 December 2011)

Abstract

This communication presents a comparison of two cases to study the process of laser beam propagation and Stimulated Brillouin Scattering (SBS) in laser plasma interaction. These two cases are, with imposing the restriction of paraxial approximation on the laser beam and, relaxing this restriction up to a certain extent. In this work, the study done by Sharma *et al.* (2009) using paraxial approximation is extended by taking contribution of the off-axial rays in the laser beam profile. The spitted profile of the laser beam is obtained due to uneven focusing of the off-axial rays and its effect on localization of the ion acoustic wave (IAW) has been studied. Including the off-axial part of the laser beam semi-analytical solution of the nonlinear coupled IAW equation has been found and this is examined that off-axial part affects background densities. The nonlinear coupling between the laser beam and IAW is severely affected by modified profile of the laser beam. Further, it is investigated that the SBS is also influenced by this coupling process. Therefore, the reflectivity of SBS has been compared with and without contribution of off-axial rays. A notable change is found in the magnitude of SBS reflectivity in modified-paraxial case in comparison to the paraxial case.

Keywords: Ion acoustic wave; Off-axial rays; Paraxial approximation; Stimulated Brillouin scattering

1. INTRODUCTION

The efficient laser-plasma coupling opens the way for various exciting laser-plasma applications like particle acceleration (Bari *et al.*, 2010) and laser fusion (Badiei *et al.*, 2010) radiation sources (Yang *et al.*, 2010; Badziak *et al.*, 2010). All these need an efficient coupling between laser and plasma and instabilities are fundamental issues in the laser-plasma coupling. It is seen that, in the underdense region, large scattering (Starodub *et al.*, 2010) of the laser can occur provided the laser power go beyond a certain threshold value; the threshold power is often exceeded in laser plasma experiments. In such cases, SBS (Huller *et al.*, 2008; Hasi *et al.*, 2008; Kappe *et al.*, 2007; Wang *et al.*, 2009) is of the special interest since it leads to large reflection losses. SBS is a parametric instability corresponding to the decay of an incident electromagnetic pump wave into an ion sound wave, and a second electromagnetic wave with lower frequency propagating in different direction. Although SBS has been the subject of extensive studies, both theoretically and experimentally, but many features of the experimental results do not agree with the theoretical prediction. These include low levels of SBS scattered light (Rozmus *et al.*, 1987). The theoretical analysis predicts high nonlinear reflectivity, but the laboratory experiments show that the reflectivity is some what lesser than the theoretical prediction (Baldis *et al.*, 1993). To resolve the discrepancy between theoretical expectations and experimental (Gao *et al.*, 2010) results, nearly all of the theoretical studies are focused with the saturation effects of SBS-driven IAW.

Most of the work on SBS deals with the propagation and transmission of laser beams in the paraxial approximation, because in the majority of cases, the divergence angles of the investigated laser beams are very small, and the beam widths of the investigated laser beams are far greater than the wavelength. Therefore, the paraxial wave equation gives an accurate description for wave beams near the axis as long as the beam width remains larger than the radiation wavelength λ throughout the propagation. However, in

Address correspondence and reprint requests to: Prerana Sharma, Physics Department, Ujjain Engineering College, Ujjain, M. P. 465010, India. E-mail: preranaiitd@rediffmail.com

some experimental situations, it is necessary to go beyond the paraxial approximation, like the use of diffractive optical elements that present small features or of tightly focusing laser beams to reach the nonlinear range of intensities may lead to optical fields that cannot be described within the paraxial approximation. In addition to that, recent advances in laser technology, based on the chirped pulse amplification technique, make intensities greater than 10^{18} W/cm^2 available for experiments. In these experiments, the laser beam power can be 1000 times larger than the critical value and one can expect multiple filamentation, focusing up to the point where the paraxial approximation breaks down in every filament and radiation scatters.

In this work, we examined the ponderomotive self focusing/filamentation of the laser beam with paraxial and modified paraxial approximation. The paraxial approximation has been modified by including fourth power of radial distance r. The higher order terms in the expansion of dielectric constant and eikonal have been taken into account. The laser intensity profile and other relevant quantities of plasma were also expended and it makes a significant difference in the study of propagation of laser beam in plasma (Liu & Tripathi). It is observed that in extended paraxial case, the filaments of the laser beam have been spitted and these modified structures affects the IAW generation. Therefore, SBS has been studied for both paraxial and modified paraxial cases and it is observed that in presence of off-axis part reflectivity of SBS is affected significantly.

The outline of this work is as follows: In Section 2, we have given the expression for the beam width parameter of the high power laser beam and modified equations for the excitation of the IAW when ponderomotive nonlinearity is operative by including the extended paraxial contribution. In Section 3, the basic equations that govern the dynamics of SBS process are given by considering the modified paraxial approximation. The SBS reflectivity has been compared for both paraxial and extended paraxial case in this section. Discussion of the results is presented in Section 4. The conclusions are given in the last section.

2. PROPAGATION OF LASER BEAM AND EXCITATION OF IAW

A high power Gaussian laser beam (pump) of frequency ω_0 and wave number k_0 is assumed to be propagating in hot collisionless homogeneous plasma along the z axis. The wave equation governing the electric field of the laser beam in plasma can be written as

$$\nabla^2\vec{E} = \frac{1}{c^2}\frac{\partial^2\vec{E}}{\partial t^2} + \frac{4\pi}{c^2}\frac{\partial\vec{J}}{\partial t}, \tag{1}$$

where $\vec{J}$ is the high frequency current density vector, further assuming the variation of electric field $\vec{E}$ of the laser beam as

$$\vec{E} = E_0(r, z)e^{-ik_0S_0(r,z)}, \tag{2}$$

with

$$k_0 = \frac{\omega_0}{c}\left(1 - \frac{\omega_p^2}{\omega_0^2}\right)^{1/2} = \frac{\omega_0}{c}\sqrt{\varepsilon_0}, \tag{3}$$

where E_0 is a complex function of space, S_0 is the eikonal, ϵ_0 is the linear part of the plasma dielectric constant. Substituting the value of j in the Eq. (1) and separating the real and imaginary parts of the resulting equation, we solve the real part equation by assuming E_0 and S_0 (by including the r^4 coefficients) in the extended paraxial approximation as, following (Akhmanov *et al.*, 1968; Sodha *et al.*, 1976; Sharma *al.*, 2009)

$$E_0^2 = \frac{E_{00}^2}{f_0^2}\left(1 + \frac{\alpha_{00}r^2}{r_0^2f_0^2} + \frac{\alpha_{02}r^4}{r_0^4f_0^4}\right)e^{-r^2/r_0^2f_0^2}, \tag{4}$$

$$S_0 = S_{00} + \frac{S_{02}r^4}{r_0^4} \; with \; S_{00} = \frac{r^2}{2f_0}\frac{df_0}{dz}, \tag{5}$$

where E_{00} is the axial amplitude, α_{00} and α_{02} are the coefficients of r^2 and r^4, respectively, and S_{00} and S_{02} both are the slowly varying function of r and z, using the normalized distance $\xi = zc/\omega_0r_0^2$, the laser beam width parameter f_0 governed as (Sharma *et al.*, 2007)

$$\frac{d^2f_0}{d\xi^2} = \frac{1}{f_0^3}\left(8\alpha_{02} + 1 - 3\alpha_{00}^2 - 2\alpha_{00}\right) - \left(\frac{3}{4}\frac{m_e}{m_i}\alpha E_0^2\right) \frac{\omega_p^2}{\omega_0^2}\frac{R_{d0}^2}{\varepsilon_0r_0^2f_0^3}(\alpha_{00} - 1)\exp\left(\frac{3}{4}\frac{m_e}{m_i}\frac{\alpha E_0^2}{f_0^2}\right), \tag{6}$$

with the following equations (Sharma *et al.*, 2007)

$$\frac{\partial S_{02}}{\partial z} = \frac{9m_e\omega_p^2\alpha_{00}E_{00}^2}{16m_ic^2k_0^2f_0^6}(1 - 2\alpha_{00} + 2\alpha_{02}) - \frac{1}{k_0^2r_0^2f_0^6} \left(2\alpha_{02} + \alpha_{00}^2 + 7\alpha_{02}\alpha_{00} - \alpha_{00}^3\right) \tag{7}$$

$$\frac{\partial\alpha_{00}}{\partial z} = -\frac{16S_{02}f_0^2}{r_0^2}, \tag{8}$$

$$\frac{\partial\alpha_{02}}{\partial z} = 8(1 - 3\alpha_{00})\frac{S_{02}f_0^2}{r_0^2}, \tag{9}$$

where $R_{d0} = k_0r_0^2$, $\xi = z/R_{d0}$. Eq. (4) gives the intensity profile of the laser beam in the plasma along with the radial direction when ponderomotive nonlinearity is operative. Numerical computation of Eq. (4) has been performed with the help of Eqs. (6)–(9).

When laser beam propagates in the plasma, its nonlinear interaction with the seed of IAW excites IAW. The excitation process of this IAW is investigated in the presence of the laser

https://doi.org/10.1017/S026303461100084X Published online by Cambridge University Press

beam having a modified profile. Combining the standard fluid equations we get the general equation governing the ion density variation as

$$\frac{\partial^2 n_{is}}{\partial t^2} + 2\Gamma_i \frac{\partial n_{is}}{\partial t} - c_s^2 \nabla^2 n_{is} + k^2 c_s^2 \left[-1 + \left(1/1 + k^2 \lambda_d^2 \left(\frac{N_{0e}}{N_{00}} \right)^{-1} \right) \right] n_{is} = 0, \tag{10}$$

The solution of the above equation can be written as

$$n_{is} = n(r, z) \exp\{i[\omega t - k(z + S(r, z))]\}, \tag{11}$$

with the Debye length λ_d as

$$\lambda_d = \left(k_\beta T_0 / 4\pi N_{00} e^2 \right)^{1/2}, \tag{12}$$

where Γ_i Landau damping coefficient for IAW, n is the real function of r and z, T_0 is the equilibrium temperature of the plasma, N_{0e} is the electron concentration in the presence of the laser beam, N_{00} is the electron density in the absence of the beam, k_β is the Boltzman's constant, and $c_s = (k_\beta T_e / M)^{1/2}$ is the speed of the IAW. The wave number k of the IAW satisfy the following dispersion relation in the presence of laser beam

$$\omega^2 = \frac{k^2 c_s^2}{1 + k^2 \lambda_d^2 \left(N_{0e} / N_{00} \right)^{-1}}. \tag{13}$$

Following Sharma *et al.* (2009) and Sharma, P. *et al.* (2009), we assume the initial radial variation of IAW density perturbation to be Gaussian, substituting (11) in (10) and the solution of the resulting equation at finite z may be written as

$$n^2 = \frac{n_0^2}{f^2} \left(1 + \frac{\alpha_{0i} r^2}{a^2 f^2} + \frac{\alpha_{2i} r^4}{a^4 f^2} \right) \exp\left(- \frac{r^2}{a^2 f^2} - k_{id} z \right), \tag{14}$$

and

$$S = S_{0i} + \frac{S_{2i} r^4}{a^4} \; with \; S_{0i} = \frac{r^2}{2f} \frac{df}{dz}, \tag{15}$$

where $k_{id} = \Gamma_i \omega / k c_s^2$ is the damping factor, a is the initial beam width of the acoustic wave, coefficients α_{0i}, etc. functions same as α_{00} etc. functions in the previous section and f is a dimensionless beam width parameter of IAW governed as (Sharma, P. *et al.*, 2009)

$$\frac{\partial^2 f}{\partial \xi^2} = \frac{R_{d0}^2}{R_d^2 f^3} \left(8\alpha_{2i} + 1 - 3\alpha_{0i}^2 - 2\alpha_{0i} \right) - \left(\frac{3}{4} \alpha \frac{m}{M} E_{00}^2 \frac{f}{f_0^4} \right) \frac{R_{d0}^2 k^2 \lambda_d^2}{r_0^2 \left(1 + k^2 \lambda_d^2 \right)^2} (\alpha_{0i} - 1) \exp\left(\frac{3}{4} \alpha \frac{m}{M} \frac{E_{00}^2}{f_0^2} \right), \tag{16}$$

where $R_d = ka^2$ is the diffraction length of the IAW and the equations for S_{2i}, α_{0i}, α_{2i} are as follows

$$\frac{\partial S_{2i}}{\partial z} = \frac{9 m_e \omega_p^2 \alpha_{00} E_{00}^2}{16 m_i k^2 v_{th}^2 f_0^6} (1 - 2\alpha_{0i} + 2\alpha_{2i}) - \frac{1}{k_0^2 r_0^2 f_0^6} \left(2\alpha_{02} + \alpha_{00}^2 + 7\alpha_{02}\alpha_{00} - \alpha_{00}^3 \right), \tag{17}$$

and the coefficient α_{0i} and α_{2i} as

$$\frac{\partial \alpha_{0i}}{\partial z} = - \frac{16 S_{2i} f^2}{a^2}, \tag{18}$$

$$\frac{\partial \alpha_{2i}}{\partial z} = 8(1 - 3\alpha_{0i}) \frac{S_{2i} f^2}{a^2}. \tag{19}$$

Eq. (14) represents the density profile of IAW in the plasma when the coupling between laser beam and IAW is taken into account.

We have solved Eq. (14) numerically with the help of Eq. (16)–(19) to obtain the density perturbation at finite z. The result is shown in Figure 3, for typical laser parameters given in the discussion section, we have used in previous section. It is evident from the figure that the IAW gets excited due to nonlinear coupling with the high power laser beam because of the ponderomotive nonlinearity.

The nonlinear evolution of IAW may play an important role in SBS process. Stimulated scattering always involves a pump laser beam and a frequency-shifted scattered wave, coupled by either molecular vibrational transitions (Raman) or acoustic waves (Brillouin). SBS is mainly driven by the acoustic waves excited by an intense laser pulse.

Here, we are considering the special case where the restriction on laser beam profile and therefore off-axial rays are also taking part in the propagation. Due to the presence of the off-axial rays, the profile of the laser beam has been modified. Further, the modified profile of the laser beam affects the amount of energy scattered by the IAW and hence SBS. Therefore, it is necessary to model the interplay between SBS and the modified laser beam profile, which has not been addressed so far. In the next section, we develop the theory of SBS in the presence of modified profile of laser beam due the contribution of the off-axial rays.

3. FORMULATION: STIMULATED BRILLOUIN SCATTERING

The total electric field E_T, may be written as the sum of the electric field E of the pump laser beam andE_S, the electric field of the scattered wave, i.e.,

$$E_T = E \exp(i\omega_0 t) + E_S \exp(i\omega_S t) \tag{20}$$

E_S arises on account of scattering of the pump beam off the IAW, i.e., Brillouin scattering. The vector E_T satisfies the

https://doi.org/10.1017/S026303461100084X Published online by Cambridge University Press

wave equation

$$\nabla^2 E_T - \nabla(\nabla \cdot E_T) = \frac{1}{c^2}\frac{\partial^2 E_T}{\partial t^2} + \frac{4\pi}{c^2}\frac{\partial J_T}{\partial t}, \tag{21}$$

where J_T is the total current density vector in the presence of the high frequency electric field E_T. Equating the zero-th order terms in above equation, one obtains equation for the field inside the plasma i.e.,

$$\nabla^2 E + \frac{\omega_0^2}{c^2}\left(1 - \frac{\omega_p^2}{\omega_0^2}\frac{N_{0e}}{N_0}\right)E = 0,$$

and equating the terms at scattered frequency we get

$$\nabla^2 E_S + \frac{\omega_S^2}{c^2}\left(1 - \frac{\omega_p^2}{\omega_S^2}\frac{N_{0e}}{N_0}\right)E_S = \frac{1}{2}\frac{\omega_p^2}{c^2}\frac{\omega_S}{\omega_0}\frac{n^*}{N_0}E. \tag{22}$$

In solving Eq. (22), the term $\nabla\ (\nabla \cdot E)$ may be neglected in the comparison to the $\nabla^2\ E_S$ term. Let the solution of Eq. (22) i.e., E_S is the electric field of the scattered wave

$$E_S = E_{S0}(r, z)e^{+ik_{s0}z} + E_{S1}(r, z)e^{-ik_{S1}z}, \tag{23}$$

and

$$E_{S0} = E_{S00}e^{ik_{S0}S_s},$$

where

$$k_{S0}^2 = \frac{\omega_S^2}{c^2}\left(1 - \frac{\omega_p^2}{\omega_S^2}\right) = \frac{\omega_S^2}{c^2}\varepsilon_{S0}, \tag{24}$$

and k_{S1} and ω_S satisfy the phase matching conditions

$$\omega_S = \omega_0 - \omega, \quad k_{S1} = k_0 - k. \tag{25}$$

Following (Sharma *et al.*, 2009) and assuming the solution as

$$E_{S00}^2 = \frac{B'^2}{f_S^2}\left(1 + \frac{\alpha_{0s}r^2}{b_0^2 f_S^2} + \frac{\alpha_{2s}r^4}{b_0^4 f_S^4}\right)\exp\left(-\frac{r^2}{b_0^2 f_S^2}\right). \tag{26}$$

$$S_s = S_{0s} + \frac{S_{2s}r^4}{b_0^4}\ \textit{with}\ S_{0s} = \frac{r^2}{2f_s}\frac{df_s}{dz}, \tag{27}$$

where b_0 is the initial beam width of the scattered wave, E_{S0} (r,z) and E_{S1} (r,z) are the slowly varying complex function of r and z, and the coefficients α_{0s}, etc. functions same as α_{00} etc. functions in the previous section. We get the equation of the spot size of scattered wave as (Sharma *et al.*, 2009)

$$\frac{d^2 f_s}{d\xi^2} = \frac{R_{d0}^2}{R_{ds}^2 f_s^3}\left(8\alpha_{2s} + 1 - 3\alpha_{0s}^2 - 2\alpha_{0s}\right) - \frac{\omega_p^2}{\omega_s^2\varepsilon_{S0}}\left(\frac{3}{4}\alpha\frac{m_e}{m_i}E_{00}^2\right)\frac{f_s}{f_0^4}\frac{R_{d0}^2}{r_0^2}(\alpha_{0s} - 1)\exp\left(-\frac{3}{4}\alpha\frac{m_e}{m_i}\frac{E_{00}^2}{f_0^2}\right), \tag{28}$$

with

$$\frac{\partial S_{2s}}{\partial z_c} = \frac{9m_e\omega_p^2\alpha_{00}E_{00}^2}{16m_i k_0^2\omega_s^2 f_0^6}(1 - 2\alpha_{0s} + 2\alpha_{2s}) - \frac{1}{k_0^2 b_0^2 f_0^6}\left(2\alpha_{02} + \alpha_{00}^2 + 7\alpha_{02}\alpha_{00} - \alpha_{00}^3\right), \tag{29}$$

$$\frac{\partial \alpha_{0S}}{\partial z_c} = -\frac{16S_{2S}f_S^2}{b_0^2}, \tag{30}$$

$$\frac{\partial \alpha_{2S}}{\partial z_c} = 8(1 - 3\alpha_{0S})\frac{S_{2S}f_S^2}{b_0^2}, \tag{31}$$

where $R_{dS} = k_{S0}\ b_0^2$ is the diffraction length of the scattered radiation.

The expressions for B' and b_0 may be obtained on applying suitable boundary conditions $E_S = E_{S0}\exp\ (ik_{S0}\ z) + E_{S1}\exp\ (-ik_{S1}\ z) = 0\ at\ z = z_c$; here z_c is the point at which the amplitude of the scattered wave is zero. This immediately yields (Sharma *et al.*, 2009)

$$B' = -\frac{1}{2}\frac{\omega_p^2}{c^2}\frac{\omega_S}{\omega_0}\frac{n_0}{N_{00}}\frac{E_{00}f_S(z_c)}{f(z_c)f_0(z_c)} \frac{\left(1 + \frac{\alpha_{0i}r^2}{a^2f^2} + \frac{\alpha_{2i}r^4}{a^4f^2}\right)^{1/2}\left(1 + \frac{\alpha_{00}r^2}{r_0^2f_0^2} + \frac{\alpha_{02}r^4}{r_0^4f_0^4}\right)^{1/2}}{\left(1 + \frac{\alpha_{0s}r^2}{b_0^2f_s^2} + \frac{\alpha_{2s}r^4}{b_0^4f_s^4}\right)^{1/2}}. \frac{\exp(-k_i z_c)}{\left[k_{S1}^2 - k_{S0}^2 - \frac{\omega_p^2}{c^2}\left(1 - \frac{N_{0e}}{N_{00}}\right)\right]} \frac{\exp[-i(k_{S1}z_c + k_0 S_0)]}{\exp[i(k_{S0}S_s + k_{S0}z_c)]}, \tag{32}$$

With condition $\frac{1}{b_0^2f_s^2} = \frac{1}{r_0^2f_0^2} + \frac{1}{a^2f^2}$.

here $k_0^2 = \omega_0^2/c^2(1 - \omega_p^2/\omega_0^2) = \omega_0^2/c^2\varepsilon_0$, $k_{S0}^2 = \omega_S^2/c^2(1 - \omega_p^2/\omega_S^2) = (\omega_S^2/c^2)\varepsilon_{S0}$ and k_{s1} and ω_s satisfy the matching conditions $\omega_S = \omega_0 - \omega\ \ k_{S1} = k_0 - k$. The reflectivity is defined as the ratio of scattered flux and incident flux, $R = (|\ E_S\ |^2\ /\ |\ E_{00}\ |^2)$. By following (Sharma *et al.*, 2009), we get

$$E_S E_S^* = E_{S0}E_{S0}^* + E_{S0}E_{S1}^*\exp[i(k_{S0} + k_{S1})z] + E_{S1}E_{S0}^*\exp[-i(k_{S0} + k_{S1})z] + E_{S1}E_{S1}^*,$$

https://doi.org/10.1017/S026303461100084X Published online by Cambridge University Press

and

$$R = \frac{1}{4}\left(\frac{\omega_p^2}{c^2}\right)^2\left(\frac{\omega_s}{\omega_0}\right)^2\left(\frac{n_0}{N_{00}}\right)^2 \frac{1}{\left[k_{s1}^2 - k_{s0}^2 - \frac{\omega_p^2}{c^2}\left(1-\frac{n_0}{N_{00}}\right)\right]^2} \left[\begin{array}{l} \frac{f_S^2(z_c)}{f^2(z_c)f_0^2(z_c)}\frac{1}{f_S^2}\exp\left(-2k_i z_c - \frac{r^2}{b_0^2 f_s^2}\right) \\ + \frac{1}{f^2 f_0^2}\exp\left(-\frac{r^2}{a^2 f^2} - \frac{r^2}{b_0^2 f_0^2} - 2k_i z\right) \\ + \frac{1}{2}\frac{1}{ff_0 f_s}\frac{f_s(z_c)}{f(z_c)f_0(z_c)}\exp\left(-\frac{r^2}{2b_0^2 f_s^2} - \frac{r^2}{2a^2 f^2} - \frac{r^2}{2r_0^2 f_0^2}\right) \\ .\exp\left\{-k_i(z+z_c)\right\}\cos\left\{(k_{S0}+k_{S1})(z-z_c)\right\} \\ \times \frac{\left(1+\frac{\alpha_{0i}r^2}{a^2f^2}+\frac{\alpha_{2i}r^4}{a^4f^2}\right)^{1/2}\left(1+\frac{\alpha_{00}r^2}{r_0^2f_0^2}+\frac{\alpha_{02}r^4}{r_0^4f_0^4}\right)^{1/2}}{\left(1+\frac{\alpha_{0s}r^2}{b_0^2f_s^2}+\frac{\alpha_{2s}r^4}{b_0^4f_s^4}\right)^{1/2}} \end{array}\right]. \quad (33)$$

SBS reflectivity is numerically calculated by using the above set of equations.

4. DISCUSSIONS

The propagation of high power laser beam has been considered in the presence of ponderomotive nonlinearity. The density of the plasma varies due to the ponderomotive force and this force is also responsible for the lowering of the channel density, therefore the refractive index increases and the laser gets focused in the plasma. Eqs. (4) and (5) describe the intensity profile of laser beam in plasma along the radial direction when the ponderomotive nonlinearity is operative. The intensity profile of the laser beam depends on the beam width f_0, and the coefficients (α_{00} and α_{02}) of r^2 and r^4 in the non-paraxial region. Eq. (6) determines the focusing/defocusing of laser beam along the distance of propagation in plasma. In Eq. (6), the first term is responsible for diffraction, while the second and third terms (nonlinear terms), on the right-hand side of the equation are responsible for the converging behavior of the beam during propagation in plasma. These three terms describe the filament formation and the laser beam propagation in plasma. Numerical evaluation of Eqs. (4) and (5) has been performed by using the typical laser beam parameters: the vacuum wavelength of the laser beam ($\lambda = 1064$ nm), the initial radius of the laser beam (15 μm), laser power flux (10^{16} W/cm^2) at plasma density, $n/n_{cr} = 0.11$ and $v_{th} = 0.1c$. For initial wave front of the beam, the initial conditions for f_0 are $f_0 = 1$ and df_0/dz at $z = 0$ and S_{00} and $S_{02} = 0$ at $z = 0$. The coupled equations have been solved with the help of Eqs (6)–(9) for an initial plane wave front of the beam and the numerical results are presented in the form of Figure 1. Figure 1a depicts the variation in laser beam intensity with normalized distance and radial distance, when the paraxial approximation is taken into consideration (by substituting α_{00} and $\alpha_{02} = 0$ in Eq. (2)). But when the values of α_{00} and α_{02} are taken into account, the coupled equations have been solved and numerical results are presented in the form of Figure 1b. Figure 1b shows the variation of the laser beam intensity with normalized distance and radial distance including the extended-paraxial contribution. It is obvious from the figure that the beam has spitted profile and in paraxial region the intensity of laser beams is maximum at $r = 0$ along the distance of propagation as $\alpha_{00} = \alpha_{02} = 0$. While in extended-paraxial region the laser intensity becomes minimum at $r = 0$, and maximum at $r = \pm$ 0.45, as also verified analytically by Eq. (4). In Figure 2, a comparison of beam width parameter has been done for both the cases paraxial and modified

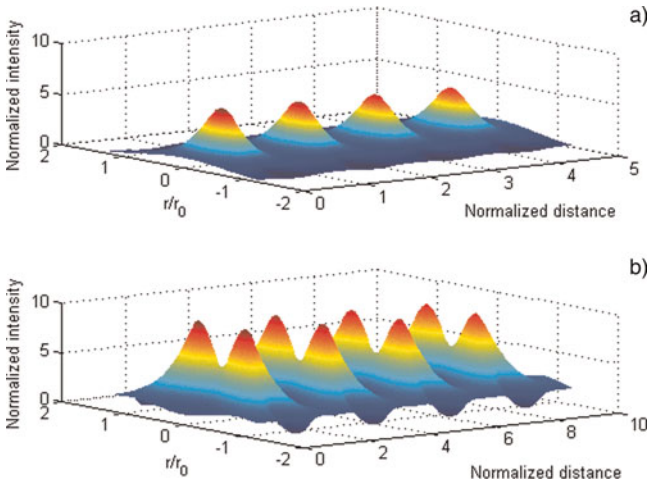

Fig. 1. (Color online) Variation of laser beam intensity with normalized distance and radial distance (**a**) in paraxial case ($\alpha_{00} = \alpha_{02} = 0$) (**b**) in extended-paraxial case ($\alpha_{00} = \alpha_{02} = 0$).

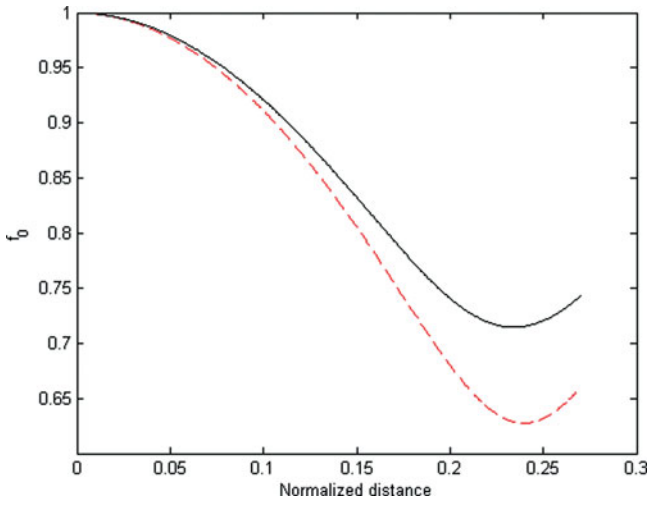

Fig. 2. (Color online) Variation in laser beam width parameter with normalized distance, where red dashed line is for on axis (paraxial) case i.e. ($\alpha_{00} = \alpha_{02} = 0$) and solid black line is for off-axial (extended paraxial) contribution i.e. ($\alpha_{00} \neq \alpha_{02} \neq 0$).

https://doi.org/10.1017/S026303461100084X Published online by Cambridge University Press

paraxial. It can clearly be observed from Figure 2 that focusing becomes faster in extended-paraxial case in comparison to paraxial case due to the participation of off-axis parts ($\alpha_{00} \neq \alpha_{02} \neq 0$).

When this laser beam propagates through plasma, the motion of electron will be modified according to the nonlinearity present in the plasma and will give rise to changes in the dispersion of the laser beam and nonlinear current density. Nonlinear interaction of seed IAW with the laser beam leads to its excitation. It is evident from the figure that IAW gets excited due to nonlinear coupling with high-power laser beam because of ponderomotive nonlinearity. We have solved Eq. (14) numerically with the help of all set of Eq. (16) to obtain the amplitude of the density perturbation at finite z. The results are displayed in Figure 3, for typical laser parameters as mentioned earlier. It is evident from the figure that the IAW gets excited due to nonlinear coupling with high power laser beam because of the ponderomotive nonlinearity. This coupling is so strong that the initial ion wave becomes highly localized as shown in Figure 3; it depicts that the IAW is also having the spitted profile with minimum power on the axis.

Eq. (28) expresses the beam width parameter of the scattered beam and Eq. (33) gives the reflectivity has been derived including off-axial coefficients. In order to observe the reflectivity against the distance of propagation, we have solved Eq. (33) numerically and the results are presented in the form of Figure 4, which shows the variation of the reflectivity with normalized distance with and without the contribution of the coefficients α_{00} and α_{02}. Figure 4 explicitly illustrates the comparison of reflectivity in the off-axis ($\alpha_{00} \neq \alpha_{02} \neq 0$) and on-axis cases ($\alpha_{00} = \alpha_{02} = 0$) of the laser beam. In Figure 4, the blue dotted line shows normalized reflectivity when restriction on the laser beam is relaxed while solid black line shows the same with restricted laser beam profile. It is observed that the reflectivity is about an order of magnitude lower with respect to the paraxial case and, the blue dotted lines come towards the left-hand side of the solid black line, it depicts that non-paraxial rays reflects earlier than the paraxial rays This is due to the fact that, in the modified paraxial case focusing becomes faster and hence the scattered wave also reflects earlier with respect to the paraxial case as shown in the blue dotted line.

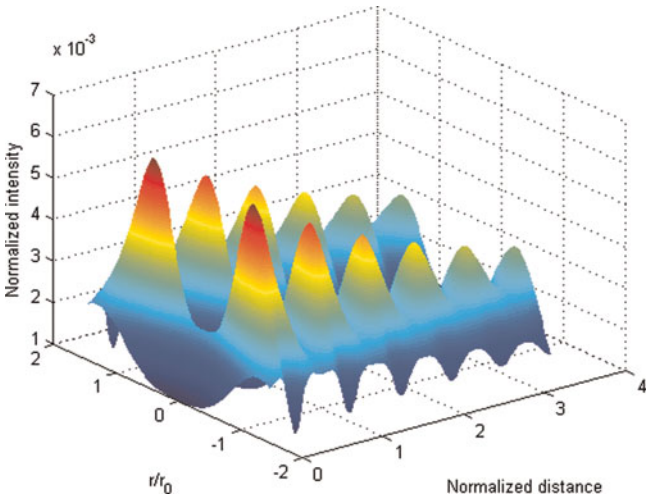

Fig. 3. (Color online) Variation of ion acoustic wave density with normalized distance and radial distance in extended — paraxial case ($\alpha_{0i} = \alpha_{2i} = 0$).

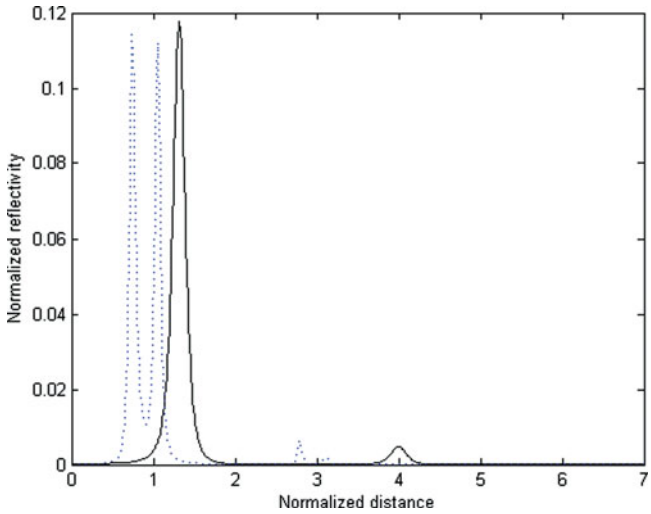

Fig. 4. (Color online) Variation in normalized reflectivity with normalized distance, where black solid line is for on axis (paraxial) case when ($\alpha_{01} = \alpha_{02} = 0$) ($\alpha_{0i} = \alpha_{2i} = 0$). ($\alpha_{0s} = \alpha_{2s} = 0$) blue dotted line is for off-axial (extended paraxial) contribution when ($\alpha_{01} \neq \alpha_{02} \neq 0$). ($\alpha_{0i} \neq \alpha_{2i} \neq 0$). ($\alpha_{0s} \neq \alpha_{2s} \neq 0$).

5. CONCLUSION

In this work, it is observed that the spitted profile of the laser beam modify the process of excitation ion acoustic wave. This modified profile of the laser beam affects the nonlinear coupling between the laser beam and IAW. Further, it is investigated that the SBS is also influenced by this coupling process, as the reflectivity depends on the density of IAW. Therefore, the reflectivity of SBS has been compared with and without contribution of off-axial rays. A considerable change is found in the level of SBS reflectivity in modified-paraxial case in comparison to the paraxial case. It is expected that these results will contribute to make smaller the discrepancy between theoretical prediction and experimental results.

ACKNOWLEDGMENT

This work was partially supported by MAPCOST, Bhopal India and DST, New Delhi India.

REFERENCES

Akhmanov, A.S., Sukhorukov, A.P. & Khokhlov, R.V. (1968). Self-focusing and diffraction of light in a nonlinear medium. *Soviet. Phys. Usp.* **10**, 609–636.

https://doi.org/10.1017/S026303461100084X Published online by Cambridge University Press

Badiei, Shahriar, Andersson Patrik, U. & Holmlid, Leif. (2010). Laser-driven nuclear fusion D + D in ultra-dense deuterium: MeV particles formed without ignition. *Laser Part. Beams* **28**, 313–317.

Badziak, J., Jaboski, S., Parys, P., Szydowski, A., Fuchs, J. & Mancic, A. (2010). Production of high-intensity proton fluxes by a 2 Nd:glass laser beam. *Laser Part. Beams* **28**, 575–583.

Baldis, H.A., Villeneuve, D.M., Fontaine, B. La., Enright, G.D., Labaune, C., Baton, S., Mounaix, Ph., Pesme, D., Casanova, M. & Rozmus, W. (1993). Stimulated Brillouin scattering in picoseconds time scale: Experiments and modeling. *Phys. Fluids B* **5**, 3319–3327.

Bari, M.A., Sheng, Z.M., Wang, W.M., Li, Y.T., Salahuddin, M., Nasim, M.H., Shabbir Naz, G., Gondal, M.A. & Zhang, J. (2010). Optimization for deuterium ion acceleration in foam targets by ultra-intense lasers. *Laser Part. Beams* **28**, 333–341.

Gao, W, Lu, Z.W., Wang, S.Y., He, W.M. & Hasi, W.L.J. (2010). Measurement of stimulated Brillouin scattering threshold by the optical limiting of pump output energy. *Laser Part. Beams* **28**, 179–184.

Hasi, W.L.J., Gong, S., Lu, Z.W., Lin, D.Y., He, W.M. & Fan, R.Q. (2008). Generation of plasma wave and third harmonic generation at ultra relativistic laser power. *Laser Part. Beams* **26**, 511–516.

Huller, S., Masson-Laborde, P.E., Pesme, D., Labaune, C. & Bandulet, H. (2008). Modeling of stimulated Brillouin scattering in expanding plasma. *J. Phys.* **112**, 022031.

Kappe, P., Strasser, A. & Ostermeyer, M. (2007). Investigation of the impact of SBS- parameters and loss modulation on the mode locking of an SBS- laser oscillator. *Laser Part. Beams* **25**, 107–116.

Rozmus, W., Sharma, R.P., Samson, J.C. & Tighe, W. (1987). Nonlinear evolution of stimulated Raman scattering in homogeneous plasmas. *Phys Fluids* **30**, 2181–2193.

Sharma, R.P., Sharma, Prerana, Rajput, Shivani & Bhardwaj, A.K. (2009). Suppression of stimulated Brillouin scattering in laser beam hot spots. *Laser Part. Beams* **27**, 619–627.

Sharma, Prerana & Sharma, R.P. (2009). Suppression of stimulated Raman scattering due to localization of electron plasma wave in laser beam filaments. *Phys. plasmas* **16**, 032301.

Sharma, R.P., Sharma, Prerana & Chauhan, P.K. (2007). Effect of laser beam filamentation on plasma wave localization and electron heating. *Phys. Plasmas* **14**, 103112.

Starodub, A.N., Borisenko, N.G., Fronya, A.A., Merkuliev, Yu.A., Osipov, M.V., Puzyrev, V.N., Sahakyan, A.T., Vasin, B.L. & Yakushev, O.F. (2010). Aerogel foil plasma: Forward scattering, back scattering, and transmission of laser radiation. *Laser Part. Beams* **28**, 371–375.

Sodha, M.S., Ghatak, A.K. & Tripathi, V.K. (1976). Self focusing of laser beams in plasmas and semiconductors. *Prog. Opt. E* **3**, 169–265.

Wang, Y.L., Lu, Z.W., He, W.M., Zheng, Z.X. & Zhao, Y.H. (2009). A new measurement of stimulated Brillouin scattering phase conjugation fidelity for high pump energies. *Laser Part. Beams* **27**, 297–302.

Yang, X.H., Ma, YY., Shao, F.Q., Xu, H., Yu, M.Y., Gu, Y.Q., Yu, T.P., Yin, Y., Tian, C.L. & Kawata, S. (2010). Collimated proton beam generation from ultraintense laser-irradiated hole target. *Laser Part. Beams* **28**, 319–325.

https://doi.org/10.1017/S026303461100084X Published online by Cambridge University Press